Examination of the Antiproliferative Activity of Iron Chelators: Multiple Cellular Targets and the Different Mechanism of Action of Triapine Compared with Desferrioxamine and the Potent Pyridoxal Isonicotinoyl Hydrazone Analogue 311[1]

Timothy B. Chaston, David B. Lovejoy, Ralph N. Watts, and Des R. Richardson[2]

The Iron Metabolism and Chelation Group, The Heart Research Institute, Camperdown, Sydney, New South Wales, 2050 Australia

ABSTRACT

Purpose: **Tumors are sensitive to iron (Fe) chelation therapy with the clinically used chelator desferrioxamine (DFO). Recently, the potent inhibitor of ribonucleotide reductase, Triapine, has entered clinical trials as an anticancer agent. This compound is a potential Fe chelator, but despite this, no investigations have examined its effect on cellular Fe metabolism. This is essential for understanding its mechanism of action and clinical effects.**

Experimental Design: **We compared the effect of Triapine with DFO, and also with the novel Fe chelator, 311, which shows marked antiproliferative activity. This latter ligand was relevant to compare, because it is tridentate like Triapine and shares structural similarity. We assessed the effects of chelators on proliferation, Fe uptake, Fe efflux, the expression of cell cycle control molecules, and iron-regulatory protein-RNA-binding activity. Redox activity was determined by ascorbate oxidation, benzoate hydroxylation, plasmid DNA degradation, and the precipitation of cellular DNA. These studies have been performed using several neuroepithelioma and neuroblastoma cell lines and a variety of normal cell types including fibroblasts, umbilical vein endothelial cells, skeletal muscle cells, monocyte-derived macrophages, and bone marrow stem cells.**

Results: **Triapine was twice as effective as DFO at mobilizing ^{59}Fe from prelabeled cells but was much less efficient than 311. In terms of preventing ^{59}Fe uptake from Tf, Triapine and DFO had similar activity, having far less efficacy than 311. All three of the chelators showed greater activity against the proliferation of neoplastic than of normal cells, the effect of 311 and Triapine being similar and these two chelators being significantly ($P < 0.0001$) more active than DFO. Complexation of Triapine with Fe had no appreciable effect on its antiproliferative activity, whereas addition of Fe totally inhibited the effects of DFO and 311. Furthermore, the Triapine Fe complex was shown to be redox active.**

Conclusion: **The cytotoxic mechanism of action of Triapine was different from that of DFO and 311, with the combined action of Fe chelation and free radical generation being involved.**

INTRODUCTION

Many *in vitro* studies as well as clinical trials have demonstrated that some tumors, particularly neuroblastoma and leukemia, are sensitive to iron (Fe) chelation therapy (1–5). The ability of chelators to inhibit growth reflects the well-known importance of Fe in a variety of crucial metabolic pathways including DNA synthesis and ATP production (6). Cancer cells, as compared with their normal counterparts, generally have higher levels of the TfR1[3] (7) and take up Fe from Tf (8, 9). The Fe requirement of tumor cells is indicated by the fact that some antibodies that block Tf binding to cells inhibit Fe uptake and cancer cell growth (10, 11). This is reflected by the ability of tumors to be radiolocalized using ^{67}Ga (12), which binds to the Tf-Fe-binding site and is delivered by receptor-mediated endocytosis (13).

The greater susceptibility of tumor cells than normal cells to Fe chelators has been seen in numerous studies with the clinically used chelator, DFO (14–20). However, DFO suffers a number of serious disadvantages including high cost, a short plasma half-life, very limited membrane permeability, poor absorption from the gut, and its requirement for long s.c. admin-

Received 7/3/02; revised 8/26/02; accepted 8/30/02.

The costs of publication of this article were defrayed in part by the payment of page charges. This article must therefore be hereby marked *advertisement* in accordance with 18 U.S.C. Section 1734 solely to indicate this fact.

[1] Supported by grants and a fellowship award from the National Health and Medical Research Council of Australia and the Australian Research Council.

[2] To whom requests for reprints should be addressed, at Children's Cancer Institute Australia, The Iron Metabolism and Chelation Program, High Street, P. O. Box 81, Sydney, New South Wales, 2050 Australia. Phone: 61-2-9382-1831; FAX: 61-2-9382-1815; E-mail: d.richardson@ccia.org.au.

[3] The abbreviations used are: Tf, transferrin; TfR, Tf receptor; DFO, desferrioxamine; RR, ribonucleotide reductase; HCT, α-(*N*)-heterocyclic carboxaldehyde thiosemicarbazone; 5-HP, 5-hydroxypyridine-2-carboxaldehyde thiosemicarbazone; HU, hydroxyurea; PIH, pyridoxal isonicotinoyl hydrazone; IRP, iron-regulatory protein; HUVEC, human umbilical vein endothelial cell; HMDM, human monocyte derived macrophage; MTT, 3-(4,5-dimethylthiazol-2-yl)-2,5-diphenyl tetrazolium; BSS, balanced salt solution; EPR, electron paramagnetic resonance; SC, supercoiled; IBE, iron-binding equivalent; GSH, glutathione; BSO, L-buthionine-[*S*,*R*]-sulfoximine; IRE, iron-responsive element; pM, log free metal ion concentration.

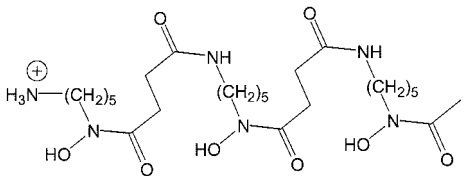

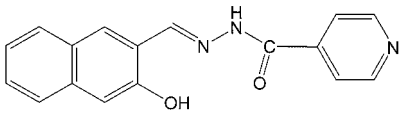

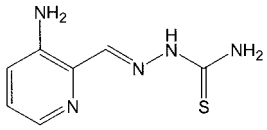

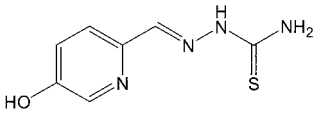

Fig. 1 Structural formulae of DFO, 2-hydroxy-1-naphthylaldehyde isonicotinoyl hydrazone (*311*), Triapine (3-aminopyridine-2-carboxaldehyde thiosemicarbazone), and 5-HP.

istration (12–24 h/day, 5–6 times/week; Ref. 6). In some cases, this has led to poor antitumor activity (6). Hence, additional studies are necessary to develop more effective ligands as anticancer agents.

Iron is a useful target because of its important role in the active sites of a range of proteins. These molecules include RR, which is critical for DNA synthesis (21, 22). RR consists of two subunits, an R1 subunit, which is involved in the binding of ribonucleotides and allosteric effectors, and an R2 subunit, which contains a tyrosyl radical that is stabilized by Fe (21). The Fe in the R2 subunit is essential for catalytic activity and is an obvious target for chemotherapeutic agents. Indeed, comparing several key enzymes, RR shows the greatest increase of activity in neoplastic tissues compared with their normal counterparts (23–26).

Investigations by Sartorelli and others (27–30) have demonstrated that the HCT chelators are among the most efficient RR inhibitors identified. One of the most active of these ligands is 5-HP (Fig. 1; Ref. 31). However, this drug was glucuronidated and rapidly excreted (32, 33). New HCTs have been developed that are resistant to glucuronidation and rapid elimination, a good example being 3-aminopyridine-2-carboxaldehyde thiosemicarbazone (Triapine; Fig. 1; Refs. 28, 34).

Triapine has recently been examined in a Phase I clinical trial, and has shown impressive results (28). For instance, this ligand shows selective antitumor activity and is fully inhibitory to cancer cells that show resistance to HU (28, 35). Although other thiosemicarbazones effectively bind Fe and result in Fe excretion in humans (32, 33), there have been no studies to investigate the effects of Triapine on Fe metabolism at the cellular or molecular level. Such experiments on this drug are important, considering current clinical trials and the possible side effects of Triapine treatment.

In the present study, we examined the Fe chelation efficacy and mechanism of action of Triapine compared with DFO and a novel chelator of the PIH class known as 2-hydroxy-1-napthylaldehyde isonicotinoyl hydrazone (311). This chelator has some structural similarity to thiosemicarbazones (see Fig. 1) and shows high Fe chelation efficacy and antitumor activity (36–39). We demonstrated that Triapine has activity somewhat similar to that of DFO but is far less efficient than 311. All three of the chelators increased IRP RNA-binding activity, which suggests chelation of intracellular Fe pools. Together, these results suggest that patients undergoing Triapine treatment should be monitored for Fe depletion. Our studies also indicated that the chelators act on multiple targets including RR and critical molecules involved in cell cycle progression. In addition, all chelators, but particularly 311 and Triapine, show selective antitumor activity. In contrast to DFO and 311, the antiproliferative activity of Triapine involves not only Fe chelation, but also the generation of cytotoxic free radicals via a redox-active Fe complex.

MATERIALS AND METHODS

Chelators

Chelator 311 was synthesized and characterized using standard procedures (39). DFO was purchased from Novartis (Summit, NJ). Triapine (3-aminopyridine-2-carboxaldehyde thiosemicarbazone) was a gift from Vion Pharmaceuticals Ltd (New Haven, CT). The DFO-Fe complex was prepared as described previously (40).

Antibodies

All antibodies were from Sigma Chemical Co. (St. Louis, MO) and Santa Cruz Biotechnology Inc. (Santa Cruz, CA) as described previously (41).

Cell Culture

The human SK-N-MC neuroepithelioma, MRC-5 fibroblast, and rat L8 skeletal muscle cell line were obtained from the American Type Culture Collection (Manassas, VA). The Kelly neuroblastoma cell line was from the European Collection of Cell Cultures (Salisbury, Wiltshire, United Kingdom). The human BE-2 neuroblastoma cell line was a gift from Dr. G. Anderson (The Queensland Institute of Medical Research, Brisbane, Queensland, Australia). All of the cell lines were grown in Eagle's modified MEM (Life Technologies, Inc., Sydney, Australia) containing 10% FCS (Life Technologies, Inc.), 1% (v/v) nonessential amino acids (Life Technologies, Inc.), 100 μg/ml streptomycin (Life Technologies, Inc.), 100 units/ml penicillin (Life Technologies, Inc.), and 0.28 μg/ml fungizone (Squibb Pharmaceuticals, Montreal, Canada). Cells were grown in an

incubator (Forma Scientific, Marietta, OH) at 37°C in a humidified atmosphere of 5% CO_2/95% air and subcultured as described previously (36). Primary cultures of HUVECs and HMDMs were prepared using standard techniques (42, 43). Bone marrow stem cell cultures were prepared using established methods (44). Cellular growth and viability were assessed by phase contrast microscopy, cell adherence to the culture substratum, and trypan blue staining.

Protein Labeling

ApoTf (Sigma) was prepared and labeled with ^{56}Fe or ^{59}Fe [as ferric chloride in 0.1 M HCl (DuPont NEN, Boston, MA)] to produce diferric Tf (^{59}Fe-Tf or ^{56}Fe-Tf; Ref. 9). Radioactive ^{59}Fe was used for Fe uptake and efflux studies, whereas nonradioactive ^{56}Fe was used in proliferation assays.

Effect of Chelators and Their Fe(III) Complexes on Cellular Proliferation

The effect of the chelators and their Fe(III) complexes on the proliferation of normal and neoplastic cells was examined using the MTT assay by the same method described previously (36, 39). The Fe(III) complexes of the chelators were prepared by adding Fe (as $FeCl_3$) to the ligands in a 1:1 ligand:metal ratio for the hexadentate chelators (*i.e.,* DFO) and a 2:1 ligand:metal ratio for the tridentate chelators (*i.e.,* 311 and Triapine). The solutions were then mixed thoroughly and incubated for 1 h at 37°C before their addition to cell cultures.

The effect of the chelators and their Fe(III) complexes on cellular proliferation were examined by seeding cells in 96-well microtiter plates at 15,000 cells/well in 100 μl of complete medium containing human diferric Tf (1.25 μM; Refs. 36, 39). This seeding density resulted in exponential growth of the cells during the duration of the assay. The cells were allowed to grow overnight, and the chelators or Fe(III) complexes were then added in 100 μl of complete medium containing unlabeled diferric Tf (1.25 μM; Refs. 36, 39). The final concentrations of the chelators or Fe(III) complexes were 0.39–25 μM. Control samples contained complete medium and diferric Tf (1.25 μM). Cells were incubated for 22–70 h at 37°C in a humidified atmosphere containing 95% air and 5% CO_2. After this incubation, 10 μl of MTT was added to each well and the plates incubated for 2 h at 37°C. The cells were then solubilized by adding 100 μl of 10% SDS-50% isobutanol in 0.01 M HCl, and the plates were then read at 570 nm on a scanning multiwell spectrophotometer (Tecan Sunrise; Tecan Austria, Salzburg, Austria). The results of the MTT assays are expressed as a percentage of the control value. For all cell types, the proliferation data obtained using the MTT assay correlated well with cell numbers estimated via microscopy (36).

Iron Uptake and Iron Efflux Experiments

The effect of chelators on ^{59}Fe uptake from ^{59}Fe-Tf and ^{59}Fe release from prelabeled cells was studied using standard procedures (36, 37). Briefly, in Fe efflux studies, cells were labeled with ^{59}Fe-Tf (0.75 μM) for 3 h at 37°C. The cells were placed on ice and washed four times with ice-cold BSS, and then reincubated for 3 h at 37°C with medium in the presence and absence of the chelators (1–50 μM). After this incubation period, the overlying medium was removed to estimate ^{59}Fe release and placed in γ-counting tubes. The cells were removed from the plates in 1 ml of BSS using a plastic scraper and were added to other counting tubes. Radioactivity was measured using a gamma counter with background correction (LKB 1282; Compugamma, Turku, Finland). The percentage of ^{59}Fe released from the cells was then calculated.

The effect of the chelators on ^{59}Fe uptake from ^{59}Fe-Tf was assessed using established methods (36, 37). Briefly, cells were incubated with ^{59}Fe-Tf (0.75 μM) in the presence and absence of the chelator (1–50 μM) for 3 h at 37°C. The cells were then placed on ice, the overlying medium aspirated, and the cell monolayer washed four times with ice-cold BSS. The cells were then removed from the plates in 1 ml of BSS and placed into γ-counting tubes to assess cellular ^{59}Fe.

IRP Gel-Retardation Assay

The gel-retardation assay was used to measure the interaction between the IRPs and iron-responsive element using established techniques (45, 46), as described in a previous investigation from our laboratory (38). Briefly, the IRE-protein complexes were analyzed in 6% nondenaturing polyacrylamide gels at 4°C. In parallel experiments, samples were treated with β-mercaptoethanol at a final concentration of 2%, before the addition of the IRE probe to allow full expression of IRE-binding activity. The IRE-protein complexes were quantified by scanning densitometry.

EPR Spectroscopy Measurement of RR

EPR spectroscopy studies of the tyrosyl radical of RR were performed using a Bruker EMX X-band spectrometer with 100-kHz field modulation. EPR spectra were recorded at −196°C using a liquid nitrogen dewer. Spectrometer settings were gain, 1×10^6; modulation amplitude, 0.3 mT; time constant, 20.5 mS; sweep time, 20.97 mS; center field, 338 mT; field sweep width, 20 mT; microwave power, 2 mW; frequency, 9.4 GHz with 32 acquisitions averaged. Spectral manipulations were performed using the program WINEPR (47). Exponentially growing cells were incubated at 37°C for 24 h in the presence or absence of 311 or Triapine (25 μM) and harvested by centrifugation at 2000 rpm for 15 min at 4°C. The cells were frozen at −196°C and EPR spectra recorded (45). Blank spectra were subtracted after storage of samples overnight at −20°C.

Northern and Western Blot Analysis

Northern Blot Analysis. Northern blot analysis was performed by isolating total RNA using the Total RNA Isolation Reagent from Advanced Biotechnologies Ltd (Surrey, United Kingdom), as described previously (38). Briefly, RNA (15 μg) was heat denatured at 90°C for 2 min in RNA-loading buffer and loaded onto a 1.2% agarose-formaldehyde gel. After electrophoresis, RNA was transferred to a nylon membrane (GeneScreen; New England Nuclear, Boston, MA) in 10× SSC using the capillary blotting method. The RNA was then cross-linked to the membrane using a UV-cross-linker (UV Stratalinker 1800; Stratagene Ltd, La Jolla, CA).

The membranes were hybridized with probes specific for human *WAF1*, *GADD45*, *TfR1*, and β-*actin*. The *WAF1* probe

consisted of a 1-kb fragment from pSXV (ATCC Cat. no. 79928). The *GADD45* probe consisted of a 760-bp fragment from human *GADD45* cDNA cloned into pHu145B2 (kindly supplied by Dr. Albert Fornace, National Cancer Institute, Bethesda, MD). The *TfR1* probe consisted of the 2.8-kb coding region from the human *TfR1* cDNA cloned into pCD-TR1 (kindly supplied by Dr. L. C. Kühn, Swiss Institute for Experimental Cancer Research, Epalinges, Switzerland). The β-*actin* probe consisted of a 1.4-kb fragment from human β-*actin* cDNA cloned into pBluescript SK− (ATCC; Cat. no. 37997).

Hybridization of probes to membranes and their subsequent washing were performed as described previously (38). Densitometric data were collected with a laser densitometer and analyzed by Kodak Biomax I Software (Kodak Ltd, Hemel Hempstead, Hertfordshire, UK). All of the results were normalized to the β-*actin*-loading control.

Western Blot Analysis. Western blot analysis was performed by standard techniques described in our previous studies (41). Briefly, lysates were mixed with loading buffer under reducing conditions and were then added (60 μg/lane) to an SDS-polyacrylamide gel (polyacrylamide = 10%). After electrophoresis, the proteins were electroblotted for 24 h at 4°C onto a PVDF membrane (NEN, Boston, MA). The membrane was stained with Ponceau S (Sigma) to ensure that all lanes contained equal amounts of protein. As an additional check of protein loading, membranes were probed for β-actin. Membranes were then washed in PBS containing 0.1% Tween 20 (PBST; Sigma) and blocked with 6% nonfat milk and 1% BSA (Sigma) in PBS for 60 min. The membranes were then washed using three 10 min washes in PBST.

Antibodies were added to PBS containing 6% nonfat milk and 1% BSA. The antibodies were incubated with the membranes for 1.5 h at room temperature. The membranes were then washed using three 10-min washes in PBST. After washing, antimouse (0.03–0.1 μg/ml) or antirabbit (0.05–0.1 μg/ml) antibodies conjugated with horseradish peroxidase (Zymed Laboratories) were incubated with the membranes for 60 min at room temperature. After washing, the membranes were developed using the Western Blot Chemiluminescence Reagent Plus (NEN) by using a 1-min incubation and exposure to X-ray film for 30 s to 15 min. The films were scanned and montages assembled with Adobe Photoshop. All of the densitometric data were normalized to the β-actin-loading control.

Ascorbate Oxidation and Benzoate Hydroxylation Assays

These assays were performed using standard methods (48). In the ascorbate oxidation experiments, ascorbic acid (0.1 mM) was incubated in the presence of Fe(III) (10 μM; added as $FeCl_3$), citrate (500 μM), and the chelator (1–60 μM). Absorbance at 265 nm was measured after 10- and 40-min incubation at room temperature and the decrease between these time points calculated (48).

The benzoate hydroxylation assay is based on the ability of hydroxyl radicals to hydroxylate benzoate to fluorescent products (308 nm excitation and 410 nm emission; Ref. 48). Benzoic acid (1 mM) was incubated for 1 h at room temperature in 10 mM sodium phosphate (pH 7.4) with 5 mM hydrogen peroxide, the Fe chelator (3–180 μM), and ferrous sulfate (30 μM; Ref. 48).

EDTA was used as a positive control because, although it is nominally hexadentate, it is not large enough to surround the Fe atom and allows the occupation of the sixth coordination site by ascorbate or H_2O. This results in redox cycling that generates free radicals (48).

Measurement of DNA Integrity Using the Plasmid pGEM-7Z*f*(+) in the Presence of Fe and the Chelator

The effect of the chelators on the integrity of plasmid DNA was performed using the plasmid pGEM-7Z*f*(+) (Promega Inc., Madison, WI) as described previously (49). Reagents were added in the following order: purified sterile water, chelator (1, 10, and 30 μM), $FeSO_4$ (10 μM), H_2O_2 (1 mM), and plasmid DNA (10 μg/ml; Ref. 50). As controls, plasmid linearized with *Bam*H1, plasmid alone, plasmid incubated with H_2O_2, and plasmid incubated with Fe(II) and H_2O_2 were used. After migration, the DNA bands were quantified using a densitometer, and the percentage of SC plasmid DNA was calculated via the equation below. A correction factor of 1.4 was applied to account for the lower fluorescence of supercoiled (SC) forms compared with the open circular (OC) and linear (L) forms (50), as follows:

$$\%\ \mathrm{SC} = \frac{1.4 \times \mathrm{SC}}{(\mathrm{L} + \mathrm{OC} + (1.4 \times \mathrm{SC})} \times 100$$

For the ascorbate oxidation, benzoate hydroxylation, and plasmid DNA strand-break assays, we have used the term "iron-binding equivalents" (IBEs) to express our data. This was because of the different coordination modes of the ligands to Fe, *i.e.*, DFO and EDTA are hexadentate and form 1:1 ligand:Fe complexes, whereas 311 and Triapine are tridentate resulting in 2:1 ligand:Fe complexes. An IBE of 1 is equivalent to the complete filling of the coordination shell of the Fe atom by the ligand(s). Thus, for a hexadentate chelator (*i.e.*, DFO or EDTA), an IBE ratio of 1 represents 1 ligand to 1 Fe atom, whereas for a tridentate chelator (*i.e.*, Triapine or 311) it is equal to 2 ligands to 1 Fe atom. An IBE of 0.1 represents an excess of Fe to chelator, *i.e.*, 1 hexadentate chelator or 2 tridentate chelators in the presence of 10 Fe atoms. An IBE of 3 represents an excess of chelator to Fe, and is equal to 3 hexadentate chelators or 6 tridentate chelators in the presence of 1 Fe atom.

GSH Assay

Intracellular GSH was measured using 5′,5′-dithiobis-(2-nitrobenzoic acid) (Sigma; Refs. 51, 52). After incubation of cells for 24 h at 37°C with chelators or the GSH synthesis inhibitor BSO (0.1 mM), GSH was assessed. BSO is a potent and selective inhibitor of γ-glutamylcysteine synthetase that is involved in GSH synthesis (53). We previously showed that BSO at 0.1 mM markedly depletes GSH without affecting cell viability (54).

DNA Precipitation Assay

This method was adapted from Olive (55). The SK-N-MC cells were labeled with [^{3}H]thymidine (0.5 μCi/ml) for 24 h, washed three times with BSS, and treated with chelators for 24 h at 37°C. Cells were added to 0.5 ml of lysis buffer (2% SDS, 10 mM EDTA, 10 mM Tris, and 0.05 M NaOH) and mixed for 1 min

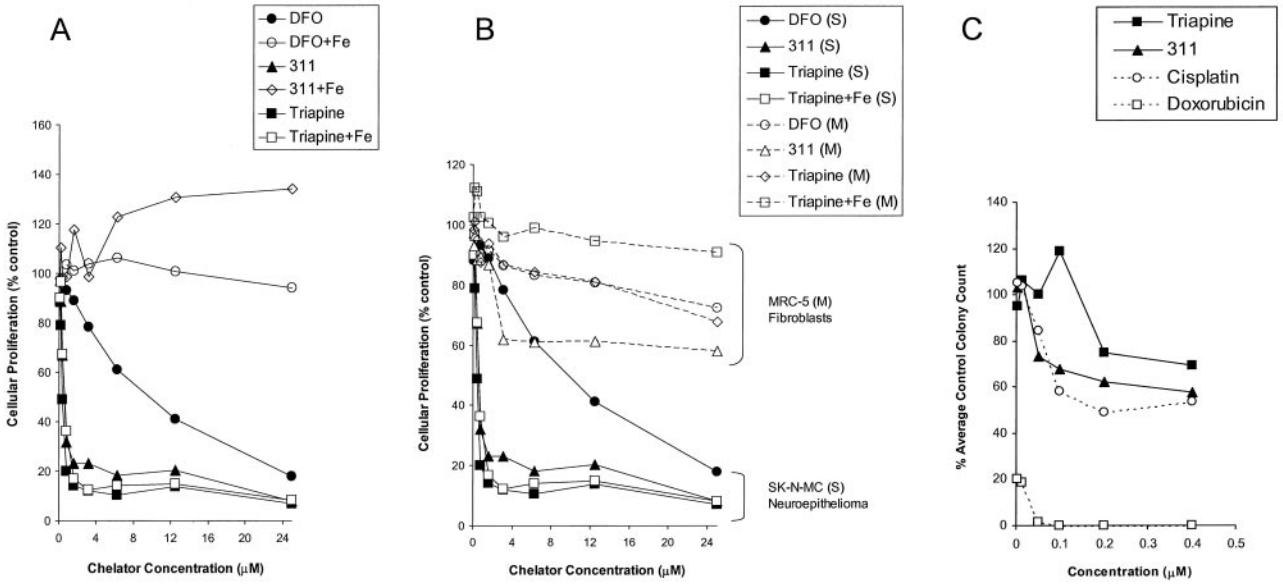

Fig. 2 The effect of DFO, 311, and Triapine, on the proliferation of neoplastic and normal cells. *A*, the effect of DFO, 311, Triapine, and their iron complexes on the proliferation of SK-N-MC neuroepithelioma cells as a function of chelator concentration. Cellular proliferation was assessed after 72 h in the presence of the compounds by the MTT assay (see "Materials and Methods" for details). *B*, the effect of DFO, 311, Triapine, and the Triapine-Fe complex on the proliferation of MRC-5 fibroblasts (*M*) compared with SK-N-MC neuroepithelioma cells (*S*). Cellular proliferation was assessed as in *A*. *C*, both 311 and Triapine have similar or less activity than cisplatin but far less activity than doxorubicin at inhibiting granulocyte-macrophage stem cell colonies from human bone marrow. Normal bone marrow stem cells were incubated for 14 days at 37°C with the agents (0.005–0.4 μM), and colonies were then counted. The results are means of three separate experiments.

Table 1 The IC_{50} values of the chelators and their iron complexes on the proliferation of neoplastic and normal cell types

The chelators and their iron complexes were incubated with cells for 72 h. At the end of this incubation period, cell density was determined by the MTT assay as described in "Materials and Methods."

	Neoplastic cells, μM			Normal cells, μM			
	SK-N-MC neuroepithelioma	BE-2 neuroblastoma	Kelly neuroblastoma	MRC-5 fibroblasts	L8 rat skeletal muscle	HUVECs	HMDMs
DFO	17.9 ± 6.9	19.5 ± 0.7	>25	>25	>25	>25	>25
DFO + Fe	>25	ND[a]	ND	>25	ND	ND	ND
311	0.50 ± 0.1	1.0 ± 0.2	1.8 ± 1.0	>25	7.2 ± 1.8	5.4 ± 0.7	20.1
311 + Fe	>25	ND	ND	>25	ND	ND	ND
Triapine	0.2 ± 0.1	0.8 ± 0.2	0.4 ± 0.1	>25	2.7 ± 1.1	9.4 ± 0.4	10.6
Triapine + Fe	0.5 ± 0.2	1.9 ± 0.7	0.9 ± 0.4	>25	ND	ND	ND

[a] ND, not determined.

on ice. To this solution, 0.5 ml of KCl (0.12 M) was added and the tubes incubated at 65°C for 10 min. Samples were then placed on ice for 5 min and centrifuged for 10 min at 3500 rpm at 4°C. The supernatant was added to 1 ml of HCl (0.05 M), and the precipitate was resuspended in 2 ml of H_2O (65°C) and added to scintillation vials. Samples were counted using a Packard Tri-Carb 2100TR Liquid Scintillation Counter (Perkin Elmer, Boston, MA). The DNA damaging agent, doxorubicin, was used as a positive control.

Statistics

Experimental data were compared using Student's paired *t* test. Results were considered statistically significant for $P < 0.05$. Results are presented as the mean, mean ± SE, or mean ± SD of three separate experiments.

RESULTS

The Effects of the Chelators on Cellular Proliferation

Considering that Triapine has entered clinical trials, it was of interest to initially determine the effect of this chelator on the proliferation of SK-N-MC neuroepithelioma cells in comparison with DFO and 311 (Fig. 1). DFO and 311 were used as the Fe chelation activity, and the antiproliferative effects of these compounds have been previously well characterized in this cell line (36–38, 41). Furthermore, DFO is a

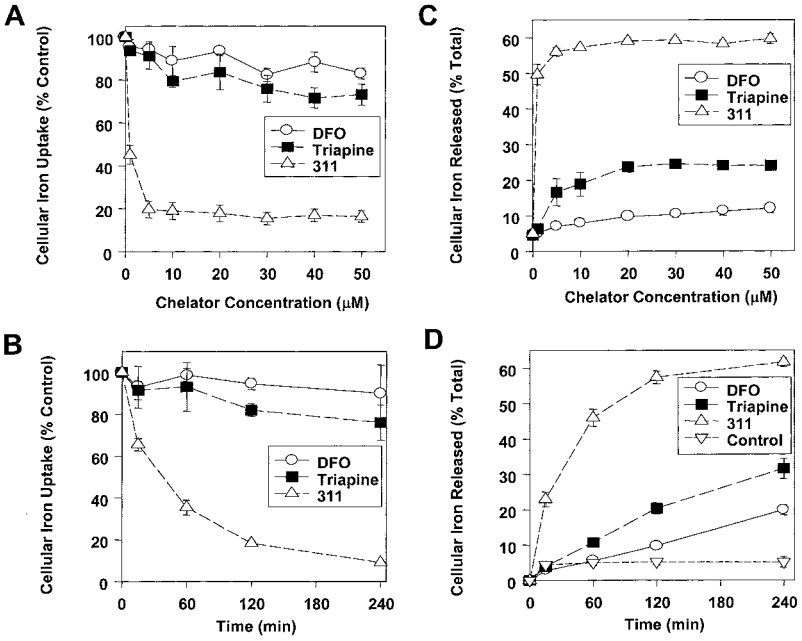

Fig. 3 The effect of chelators on inhibiting iron uptake from Tf (*A* and *B*) and increasing iron release (*C* and *D*) from SK-N-MC neuroepithelioma cells as a function of concentration and time. In *A*, cells were incubated with ^{59}Fe-Tf (0.75 μM) in the presence of the chelators (1–50 μM) for 3 h at 37°C. In *B*, cells were incubated with the chelators (50 μM) and ^{59}Fe-Tf (0.75 μM) for 1–240 min at 37°C. After incubation of the cells with ^{59}Fe-Tf and the chelators in *A* or *B*, the medium was removed and the cells washed four times on ice (see "Materials and Methods" for details). In *C* and *D*, cells were incubated for 3 h at 37°C with ^{59}Fe-Tf (0.75 μM), washed four times on ice, and then reincubated either (*C*) for 3 h at 37°C with the chelator (1–50 μM) or (*D*) for 0–240 min at 37°C with control medium or the chelator (50 μM). The supernatant was decanted from the cells and placed into γ-counting tubes. The cells were then detached from the plates to estimate cellular ^{59}Fe (see "Materials and Methods"). The results are mean ± SE from three separate experiments.

clinically used Fe chelator that has been widely examined in many studies assessing antitumor activity, whereas 311 is a ligand with pronounced anticancer activity that may have clinical potential (6, 36–39).

Both Triapine and 311 had approximately equal activity at inhibiting the growth of SK-N-MC cells, being significantly ($P < 0.0001$) more effective than DFO (Fig. 2A; Table 1). The IC_{50}s for Triapine, 311, and DFO were 0.2 ± 0.1 μM, 0.5 ± 0.1 μM, and 17.9 ± 6.9 μM (Table 1), respectively. Interestingly, the addition of Fe to Triapine had no significant ($P > 0.05$) effect on its cytotoxic activity (Table 1). This could suggest a possible role of the Fe complex in the biological activity of Triapine. This is in marked contrast to both DFO and 311, in which complexation with Fe totally prevented their cytotoxicity (Fig. 2*A*).

Additional studies were designed to determine whether any of these chelators showed selectivity for neoplastic cells compared with normal cells (Fig. 2, *B* and *C*; Table 1). Initially, we examined the effects of the chelators on the growth of SK-N-MC neuroepithelioma cells compared with MRC-5 fibroblasts. For all of the experiments, the chelators had less effect on the growth of the fibroblasts than on SK-N-MC cells (Fig. 2*B*). Particularly notable was the marked antiproliferative effects of 311 ($IC_{50} = 0.5$ μM) and Triapine ($IC_{50} = 0.2$ μM) in SK-N-MC cells and their significantly ($P < 0.0001$) lower activity in fibroblasts ($IC_{50} > 25$ μM; Fig. 2*B*; Table 1). Indeed, the selective antitumor activity of 311 and Triapine was much greater than that found for DFO (Fig. 2*B*). Additional studies with other tumor cell types (Kelly and BE-2 neuroblastoma cell lines) compared with other normal cell types (L8 skeletal muscle cells, HUVECs, and HMDMs) also showed that neoplastic cells were more sensitive to the action of Triapine and 311 than were normal cells (Table 1). Of particular relevance were the results showing that 311 and, particularly, Triapine had similar or less antiproliferative activity against normal bone marrow progenitor cells than did the cytotoxic agent cisplatin (Fig. 2*C*). In addition, the antiproliferative effects of these chelators against these normal cells were far less than that found for the widely used antitumor drug, doxorubicin (Fig. 2*C*). It is important to note that, clinically, cisplatin is not a significant myelosuppressive agent, whereas doxorubicin is. Because the inhibition of colony growth by the chelators was relatively similar to that by cisplatin (Fig. 2*C*), it can be suggested that myelosuppression with these agents may not be marked.

The Effects of Triapine, 311, and DFO on Iron Uptake from Tf and Iron Mobilization from Cells

To determine the mechanism of action of Triapine, studies were designed to determine the ability of this ligand to inhibit ^{59}Fe uptake from ^{59}Fe-Tf (Fig. 3, *A* and *B*) and increase ^{59}Fe mobilization from prelabeled SK-N-MC neuroepithelioma cells (Fig. 3, *C* and *D*). Again, DFO and 311 were used as relevant internal controls.

Iron Uptake from ^{59}Fe-Tf. In studies examining the effect of chelator concentration on ^{59}Fe uptake from ^{59}Fe-Tf, 311 was the most active compound, markedly reducing ^{59}Fe uptake to 20 ± 4% of the control value at concentrations as low as 5 μM (Fig. 3*A*). In contrast, DFO had little effect, even at the highest ligand concentration tested (Fig. 3*A*). These results with DFO and 311 are in good agreement with our previously published work (36–38). Triapine was slightly more effective than DFO but only at concentrations of 40 μM or greater (Fig. 3*A*). However, Triapine had far less activity than 311, reducing ^{59}Fe uptake from ^{59}Fe-Tf to 73 ± 5% of the control value at the highest concentration tested (*i.e.*, 50 μM; Fig. 3*A*).

Additional experiments investigated the effect of incubation time on ^{59}Fe uptake from ^{59}Fe-Tf (Fig. 3*B*). The effect of Triapine at reducing ^{59}Fe uptake was most pronounced at the

longest incubation time of 240 min, at which it reduced ^{59}Fe uptake to 76 ± 8% of the control, there being no significant difference when compared with DFO (Fig. 3*B*). Again, the most effective ligand was 311, which reduced ^{59}Fe uptake from Tf to 9 ± 1% of the control after 240 min of incubation (Fig. 3*B*).

Iron Mobilization. The effect of ligand concentration on increasing ^{59}Fe mobilization from SK-N-MC cells was examined by labeling cells with ^{59}Fe-Tf (0.75 μM) for 3 h at 37°C followed by washing and reincubation with the chelators for 3 h at 37°C (Fig. 3*C*). DFO was the least effective ligand examined, showing little effect on ^{59}Fe release from these cells. Indeed, even at 50 μM, DFO released only 12 ± 1% of cellular ^{59}Fe, whereas control medium released 5 ± 1% (Fig. 3*C*). The ^{59}Fe release induced by Triapine increased to a concentration of 20 μM and then plateaued up to 50 μM; at this concentration, the ligand was shown to mobilize 24 ± 1% of cellular ^{59}Fe (Fig. 3*C*). Hence, on a concentration basis, Triapine was approximately twice as effective as DFO in terms of inducing ^{59}Fe mobilization from SK-N-MC cells. As found previously (36, 37), 311 markedly increased cellular ^{59}Fe release from 5 ± 1% (control medium) to 50 ± 3% at a chelator concentration of 1 μM (Fig. 3*C*). The ^{59}Fe mobilization from cells mediated by 311 plateaued at a concentration of 5 μM, at which concentration 56 ± 1% of cellular ^{59}Fe was released (Fig. 3*C*).

In terms of the efficiency of ^{59}Fe mobilization, 311 again was the most effective compound, whereas Triapine was more effective than DFO at incubation times from 60–240 min (Fig. 3*D*). After an incubation of 240 min, DFO, Triapine, and 311 released 20 ± 1%, 32 ± 3%, and 62 ± 1% of cellular ^{59}Fe, respectively, whereas control medium mobilized 5 ± 1% (Fig. 3*D*).

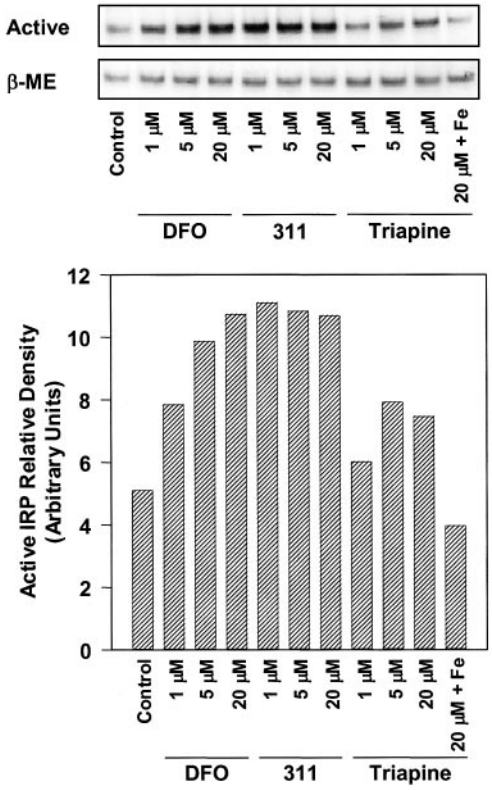

Fig. 4 The effect of chelator concentration on IRP-RNA binding activity in SK-N-MC neuroepithelioma cells. Cells were incubated with the chelators (1–20 μM) for 20 h at 37°C and IRP-RNA binding activity then assessed in the presence and absence of β-mercaptoethanol (β-*ME*; see "Materials and Methods"). Quantitation of the active IRP-RNA-binding activity via densitometry is shown below the autoradiograph. The results are a typical experiment from three performed.

The Effect of Triapine, 311, and DFO on IRP RNA-Binding Activity

To further characterize the effects of these chelators on cellular Fe metabolism, we examined their effect on the RNA-binding activity of the IRPs. The IRPs play an essential role in regulating intracellular Fe metabolism because they control the expression of a variety of molecules involved in Fe uptake (*e.g.*, TfR1) and Fe storage (*e.g.*, ferritin; reviewed in 6). There are two IRPs, IRP1 and IRP2, which, in human cells, comigrate in nondenaturing polyacrylamide gels (Fig. 4). All three of the ligands increased active IRP-RNA-binding activity as a function of chelator concentration, although Triapine was less active in this regard (Fig. 4). The Fe-complex of Triapine, in contrast to the ligand, did not increase active IRP-RNA-binding activity and, actually, slightly decreased it compared with the control (Fig. 4).

The Effect of Triapine and 311 on RR Activity

Previous studies have demonstrated that DFO inhibits RR activity because of its ability to bind cellular Fe (6, 22). In view of the differing abilities of Triapine and 311 to mobilize cellular Fe (Fig. 3, *C* and *D*), it was important to assess the effect of these chelators on RR activity. To directly determine the effect of chelators on the activity of this enzyme in intact cells, EPR spectroscopy was used. As shown in previous studies (22), the reaction of the binuclear Fe center of RR with oxygen generates a tyrosine radical that gives a characteristic EPR signal at $g = 2.0$. The presence of the tyrosyl radical is directly proportional to enzyme activity and has already been shown to give a direct measure of RR activity (22). Treatment of SK-N-MC cells for 24 h with either 311 or Triapine decreased the tyrosyl radical of RR to 48 and 61% of the control, respectively. These data indicate that despite the difference in the ability of these ligands to chelate cellular Fe (see Fig. 3), both are effective at inhibiting RR. The ability of DFO to inhibit RR activity has been well described (6, 22) and is not presented in the present study.

Effect of the Chelators on the Expression and Translation of Molecules Involved in Cell Cycle Progression and Proliferation

The effect of Triapine on the expression of cell cycle control molecules was compared with DFO and 311 (Fig. 5, *A* and *B*). The molecules examined included the retinoblastoma susceptibility gene product (pRb), the cyclins (cyclin A, E, D1, D2, and D3), and the cyclin-dependent kinases Cdk2 and Cdk4. All of these proteins play critical roles in G_1-S-phase progression and were important to assess because chelators are well known to arrest cells at this stage of the

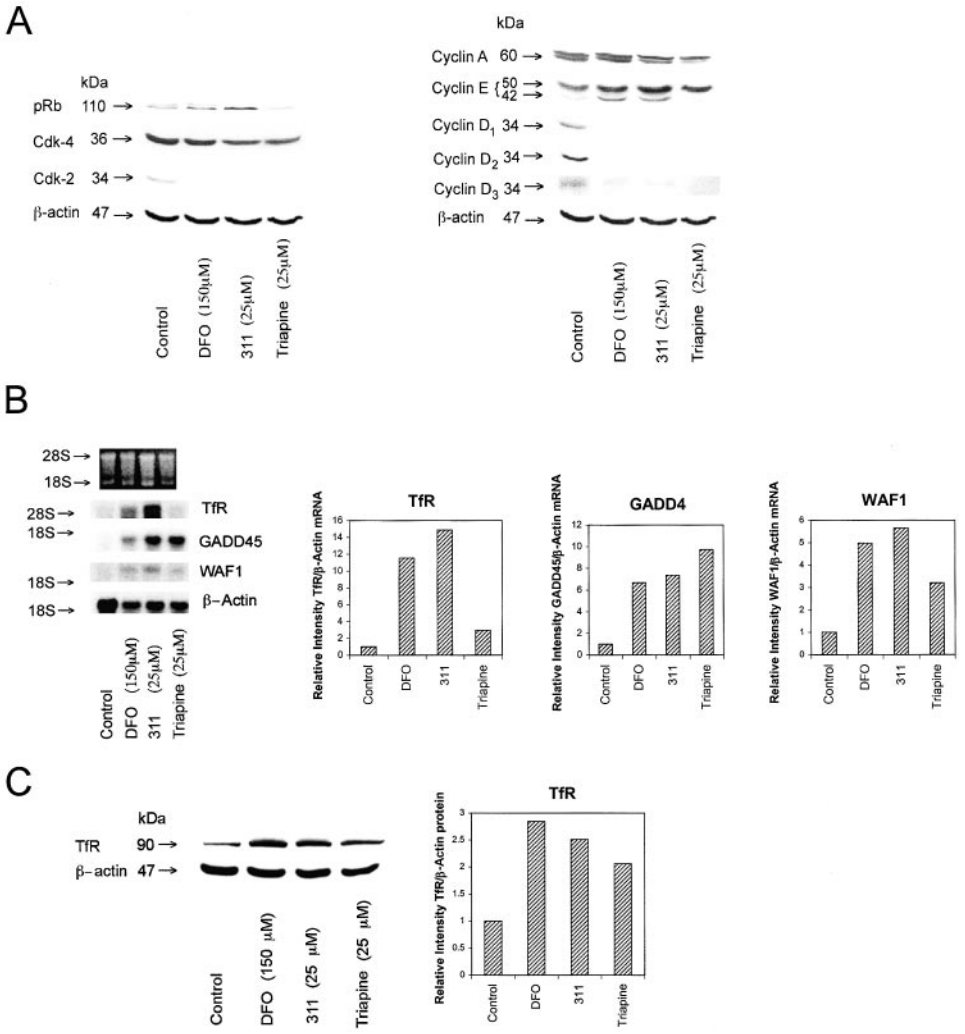

Fig. 5 The effect of the chelators on the expression of molecules involved in the cell cycle and proliferation. *A*, the effect of DFO, 311, or Triapine on the expression of the *retinoblastoma* gene susceptibility product (*pRb*), cyclin-dependent kinase 2 (*Cdk2*), Cdk4, the cyclins A, E, D1, D2, and D3. The SK-N-MC neuroepithelioma cells were incubated for 24 h at 37°C with DFO (150 μM), 311 (25 μM), or Triapine (25 μM). *B*, the effect of DFO, 311, or Triapine on the level of *TfR1*, *GADD45*, and *WAF1* mRNAs. Densitometric analysis relative to the β-actin loading control is shown to the right of the autoradiographs. Cells were treated as described in *A*, and Northern blot analysis performed (see "Materials and Methods"). *C*, the effect of DFO, 311, and Triapine on TfR1 protein levels. Cells were treated as described for *A* and *B*, and Western analysis was performed (see "Materials and Methods"). Results shown are representative of three experiments performed. *kDa*, M_r in thousands.

cycle (6). Phosphorylation of pRb by G_1 Cdk activity is critical for cell cycle progression. In SDS gels, pRb separates into two bands, the top band being the hyperphosphorylated molecule (56; see control, Fig. 5*A*). As found previously for DFO and 311 (41), these chelators and Triapine decreased phosphorylation of pRb (Fig. 5*A*). Triapine also acted to slightly decrease unphosphorylated pRb. The decrease in pRb phosphorylation may be attributable to the marked decrease in the levels of cyclin D1, D2, and D3 and Cdk2 that are found after incubation with each chelator (Fig. 5*A*). In contrast to these effects, DFO and 311 had little appreciable influence on cyclin A levels, whereas Triapine slightly decreased it. Both DFO and 311 increased the expression of the cyclin E M_r 42,000 and M_r 50,000 bands when compared with the control, whereas Triapine increased the M_r 50,000 band but had little effect on the M_r 42,000 band (Fig. 5*A*). In terms of the effects of the chelators on Cdk4 protein levels, DFO had little effect, whereas 311 and Triapine slightly reduced it (Fig. 5*A*). The effect of 311 on Cdk4 levels was somewhat variable, with no effect being observed in other experiments (data not shown).

As shown for 311 and DFO in previous studies (38), Triapine also acted to increase the expression of the mRNA levels of the *TfR1* and the cell cycle-inhibitory genes, *GADD45* and *WAF1* (Fig. 5*B*). However, whereas DFO and 311 markedly increased *TfR1* mRNA levels to 10–15-fold greater than the control, Triapine was far less effective, resulting in a 3-fold increase in *TfR1* mRNA expression over the control (Fig. 5*B*). This result with Triapine at the mRNA level was consistent with the expression of TfR1 protein that increased to a similar extent after incubation with this ligand (Fig. 5*C*). However, it is of interest to note that, whereas 311 and DFO markedly increased *TfR1* mRNA levels to 10–15-fold greater than the control (Fig. 5*B*), they increased TfR1 protein levels only 2.5–2.8-fold (Fig. 5*C*). In fact, 311 and DFO were only slightly more effective than Triapine at increasing TfR1 protein expression (Fig. 5*C*). The reason for this difference in mRNA and protein expression for 311 and DFO remains unclear at present. The effects of Triapine on ferritin protein expression were simply inversely related to that found for the TfR1, as per IRP-IRE theory (data not shown).

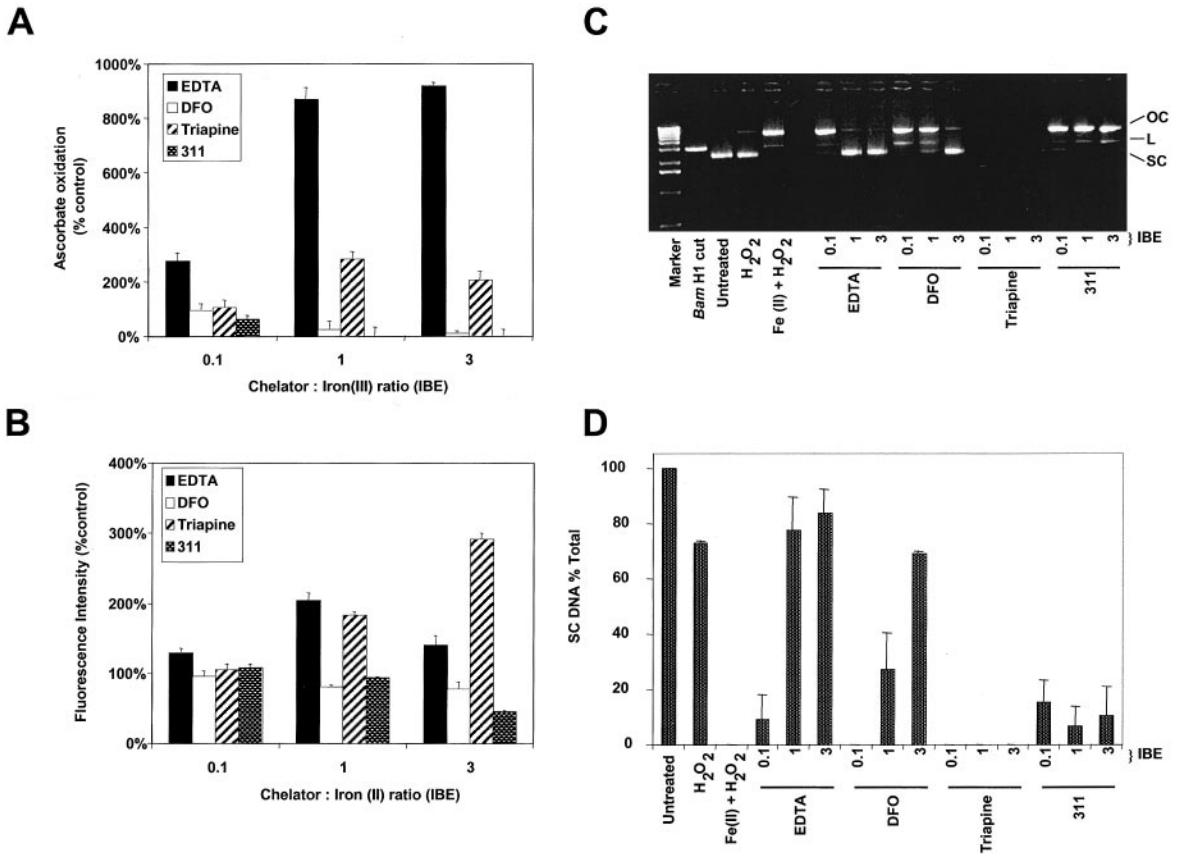

Fig. 6 Effect of the chelators on iron-mediated free-radical production as assessed by: *A*, Fe(III)-induced oxidation of ascorbate; *B*, the Fe(II)-induced hydroxylation of benzoate; and (*C* and *D*) the integrity of the plasmid pGEM-7Z*f*(+) when incubated in the presence of Fe(II) and hydrogen peroxide. Ascorbate oxidation, benzoate hydroxylation, and the integrity of plasmid DNA were assessed as described in the "Materials and Methods." *D*, densitometric analysis of the results in *C*, showing the percentage of DNA in its SC form. The results are mean ± SE of three experiments.

The Ability of Chelators to Effect Iron-dependent Free-Radical Damage

Chelators that bind Fe and then facilitate redox reactions (*e.g.*, Fenton chemistry) may cause cytotoxicity (48). This is an important component of the antitumor effects of some of the most potent chemotherapeutic agents in use (*e.g.*, doxorubicin and bleomycin; Ref. 57). In the present study, we have assessed the ability of the chelator-Fe complexes to effect Fe-mediated free radical production by using the ascorbate oxidation, benzoate hydroxylation, and plasmid DNA cleavage assays. In all of these experiments, EDTA and DFO were used as internal controls, because their effects have been well characterized (48, 58, 59).

Ascorbate Oxidation. Fig. 6*A* shows the effects of the chelators on the reducibility of Fe(III) as determined by ascorbate oxidation. The oxidation of ascorbate by EDTA was pronounced at all chelator:Fe(III) ratios (expressed as IBEs; see "Materials and Methods" for details). At IBE ratios of 0.1, 1, and 3, EDTA increased ascorbate oxidation to 276 ± 29%, 870 ± 43%, and 918 ± 14% (three experiments) of the control, respectively (Fig. 6*A*). In contrast, DFO and 311 markedly prevented ascorbate oxidation as the IBE ratio increased, reducing it to 10% of the control (DFO) or less (311) at an IBE ratio of 3. On the other hand, Triapine increased ascorbate oxidation at IBE ratios of 1 and 3 to 282 ± 28% and 203 ± 33% (three experiments) of the control, respectively (Fig. 6*A*).

Benzoate Hydroxylation. As shown previously by others (48), EDTA increased benzoate hydroxylation, particularly at IBE ratios of 1 and 3, when it was increased to 211 ± 10% and 153 ± 14% of the control, respectively (Fig. 6*B*). DFO had little effect on benzoate hydroxylation at all of the chelator: Fe(II) ratios (Fig. 6*B*), and this agreed well with previous work by others (48). This result may be explained by the low affinity of DFO for Fe(II) relative to Fe(III) (60). Experiments using 311 showed that benzoate hydroxylation was significantly inhibited only at an IBE ratio of 3 (Fig. 6*B*). At an IBE ratio of 0.1, Triapine had no effect on benzoate hydroxylation. However, when Triapine was used at IBE ratios of 1 and 3, benzoate hydroxylation increased to 183 ± 4% and 292 ± 9% of the control, respectively (Fig. 6*B*). Hence, in these experiments, when the IBE ratio was equal to 3, the ability of Triapine to hydroxylate benzoate in the presence of Fe(II) was more marked than EDTA (Fig. 6*B*).

Effect of the Chelator-Fe Complexes on Plasmid DNA Integrity. Previous studies have shown that some chelators can prevent the Fe-dependent hydroxyl radical-mediated strand

breaks in plasmid DNA (50). In the present study, we examined the ability of chelators to prevent Fe-mediated hydroxyl radical damage. Untreated plasmid or plasmid treated with H_2O_2 runs on agarose gels as a single band of DNA in its SC form (Fig. 6 *C* and *D*). Treatment of the plasmid with the restriction enzyme *Bam*H1 resulted in linear DNA. On treatment of the plasmid with Fe(II) and H_2O_2 (Fig. 6, *C* and *D*), the SC DNA was converted into the Tf state and a small amount of the linear form. This result is attributable to Fe-induced hydroxyl radical-mediated single- and double-strand breaks in DNA, respectively (Fig. 6, *C* and *D*).

Although EDTA was redox active in both the ascorbate (Fig. 6*A*) and benzoate hydroxylation assays (Fig. 6*B*), this chelator was protective of SC plasmid DNA at IBE ratios of 1 or 3 in the presence of Fe(II) and H_2O_2 (Fig. 6, *C* and *D*). This was consistent with the well-known protective effects of EDTA on DNA. Indeed, at an IBE ratio of 3, 84% of SC DNA was observed compared with only 9% at an IBE ratio of 0.1. DFO was most protective against Fe(II)- and H_2O_2-mediated plasmid damage at an IBE ratio of 3 (Fig. 6, *C* and *D*). The lower efficacy of DFO than that of EDTA to protect against Fe(II)-mediated DNA damage may again relate to the much lower affinity of DFO for Fe(II) than for Fe(III) (60). Unlike DFO and EDTA, 311 exhibited no marked ability to protect SC DNA in the presence of Fe(II) and H_2O_2 (Fig. 6, *C* and *D*), and this is probably related to the very low affinity of the PIH group of ligands for Fe(II) (60, 61). In light of these data, it should be noted that the Fe(II)-EDTA complex has a pM (a measure of ligand metal ion affinity) of 14.3, whereas that of DFO is 7.6 and PIH (a close structural analogue of 311 with identical Fe-binding sites) has a pM of 6 (pM = 6 is equivalent to undetectable binding; Refs. 60, 61). These differences in binding affinity for Fe(II) are significant and may account, in part, for the marked protective effect of EDTA, the lesser protective effect of DFO, and the fact that 311 did not prevent plasmid degradation (Fig. 6, *C* and *D*).

Interestingly, in contrast to the observations for 311 in the plasmid degradation procedure (Fig. 6, *C* and *D*), the 311-Fe complex appeared to be redox-inactive in both the ascorbate (Fig. 6A) and benzoate assays (Fig. 6B). These data are consistent with the observation that the 311-Fe complex did not inhibit cellular proliferation (Fig. 2*A*). The reason for the discrepancy between the benzoate hydroxylation and plasmid DNA assay may relate to differences in the interactions of 311 and/or Fe(II) with benzoate and DNA.

In contrast to the other chelators, Triapine resulted in marked DNA degradation in the presence of H_2O_2 and Fe(II), this reaction being so intense that no plasmid could be detected (Fig. 6, *C* and *D*). This latter effect was correlated with the ability of Triapine to cause oxidation of ascorbate (Fig. 6*A*) and to hydroxylate benzoate (Fig. 6*B*). These results, considered in conjunction with the fact that the Triapine Fe-complex maintains its cytotoxic effects (Fig. 2*A*), strongly suggest that the mechanism of cytotoxicity of this chelator is different from either DFO or 311 and involves the generation of cytotoxic free-radical species. Finally, it should be noted that all of the chelators in the absence of Fe had no effect on plasmid integrity (data not shown).

In the experiments examining ascorbate oxidation, benzoate hydroxylation, and plasmid DNA degradation, it could be suggested that the kinetics of complex formation may play a role in the assays. To determine whether this was the case, Fe complexes were preformed by incubating Fe and the chelator for 1 h in solutions degassed with N_2. Examination of these solutions using UV-Vis spectrophotometry showed that the Fe complex had formed. When these Fe complexes were compared with the usual assay procedures without preincubation of the chelators with Fe, there was no difference in the results obtained. These data indicate that the kinetics of complex formation does not play a role in the results obtained. Indeed, the capability of chelators such as EDTA to markedly inhibit plasmid DNA degradation indicates their ability to sequester Fe from DNA and prevent the formation of DNA-Fe complexes.

The Effect of Chelators on Intracellular GSH Levels and the Proportion of Precipitable DNA in SK-N-MC Cells

In additional experiments we examined the effects of incubating the chelator for 24 h on indices of redox status and DNA damage in living cells. We assessed the effects of the ligands on the major cellular reductant GSH, which is sensitive to oxidant stress. We also examined the proportion of precipitable genomic DNA in cells because this is indicative of DNA damage (55).

As a positive control in studies examining the effects of the chelators on GSH levels, we have used the specific GSH synthesis inhibitor, BSO (0.1 mM; Ref. 53), which reduced GSH levels to 41 ± 1% of the control. Both 311 (50 μM) and Triapine (50 μM) were similarly effective, reducing GSH levels to 42 ± 2% and 41 ± 4% of the control, respectively. In contrast, DFO showed far less effect even at a concentration of 100 μM, reducing GSH levels to 80 ± 5% of the control.

In the DNA precipitation assay, the DNA-damaging agent, doxorubicin (10 μM), was used as a positive control and significantly ($P < 0.0001$) reduced precipitable DNA to 22 ± 3% of the control after a 24-h incubation. Triapine significantly ($P < 0.0001$) decreased the precipitation of DNA to 65 ± 3% and 62 ± 1% of the control at a concentration of 10 and 50 μM, respectively. At a concentration of 10 μM, 311 was slightly less effective than Triapine, reducing DNA precipitation to 81 ± 4% of the control. However, at 50 μM, the activities of Triapine and 311 were very similar, 311 decreased the precipitation of DNA to 61 ± 6% of the control.

DISCUSSION

We show that the potent Fe chelator 311 demonstrates selectivity against cancer cells compared with normal cells *in vitro* (Fig. 2, *B* and *C*; Table 1). In addition, the selective antitumor activity of 311 is similar to Triapine and much greater than that of DFO. Considering the success of DFO and Triapine *in vitro*, *in vivo*, and in clinical trials (14–20, 28), this study confirms the potential of Fe chelators as antitumor agents. Furthermore, our present investigation supports the continued examination of new ligands such as 311 (36–39, 41).

To our knowledge, this study is the first to demonstrate that Triapine can act as a chelator to prevent Fe uptake from Tf (Fig. 3, *A* and *B*) and increase Fe mobilization from cells (Fig. 3, *C* and *D*). Because Triapine is undergoing clinical trials as an

antitumor agent (28), it is vital to further understand the basis of its mechanism of action. It was also important to determine the mechanism of action of Triapine in relation to the PIH analogue, 311, which demonstrates structural similarity (Fig. 1) and much greater antiproliferative activity than DFO (36–39). Surprisingly, there has been no comprehensive analysis of the effects of Triapine on Fe metabolism at the molecular or cellular level.

Our study indicates that the ability of Triapine to mobilize Fe from cells is about twice as great as that of DFO, but much less than that found for the cytotoxic Fe chelator, 311. In addition, Triapine had about the same activity as DFO at inhibiting Fe uptake from Tf, but again both of these chelators were much less efficient than was 311. Previous investigations with a related compound, namely, 2-formylpyridine thiosemicarbazone, showed that it could bind Fe (62). However, none of these latter studies assessed the effects of this agent on the cellular or molecular mechanisms involved in Fe metabolism. The extent of Fe chelation with Triapine observed in our *in vitro* studies is appreciable enough to suggest that the Fe status of patients undergoing Triapine therapy should be carefully monitored. Considering this, it is notable that another related thiosemicarbazone, namely 5-HP (Fig. 1), did increase Fe excretion from patients (33).

It was of interest to find that in contrast to the Fe complexes of DFO and 311, the Triapine-Fe complex showed cytotoxicity that was similar to the free ligand (Fig. 2A). These results suggest that the Triapine-Fe complex may play a role in Triapine cytotoxicity. Indeed, four other lines of evidence also indicated that the Triapine-Fe complex was redox active: (*a*) Triapine increased the oxidation of ascorbate in the presence of Fe(III), whereas DFO and 311 prevented it (Fig. 6*A*); (*b*) Triapine acted to increase the hydroxylation of benzoate in the presence of Fe(II), being more efficient than the positive control EDTA (Fig. 6*B*); (*c*) in contrast to DFO and 311, in the presence of Fe(II), Triapine resulted in marked plasmid DNA degradation even at very low concentrations (Fig. 6, *C* and *D*); and (*d*) incubation with Triapine resulted in depletion of the cellular reductant GSH. This latter effect was probably mediated by the localized generation of hydroxyl radicals close to DNA by the Triapine-Fe complex. These results suggest that, apart from the ability of Triapine to bind cellular Fe, the production of free radicals by the Fe complex of this ligand may also play a role in its antitumor activity. Triapine appears to mediate selective antitumor activity by forming toxic Fe complexes and thus utilizes the accumulated Fe in cancer cells as a means of imparting cytotoxicity. With this in mind, we examined whether there was antagonism between other chelators and Triapine. Interestingly, there was no effect on Triapine cytotoxicity when cells were coincubated with the Fe chelators DFO or PIH (data not shown). This suggests that the chelators may bind distinct Fe pools within cells to exert their effects.

Both Triapine and 311 caused considerable depletion of the major intracellular reductant, GSH. In addition, Triapine and 311 acted to decrease the proportion of precipitable DNA, although Triapine was more effective than 311 at low concentrations, and this was consistent with its destructive effects in the plasmid degradation assay (Fig. 6, *C* and *D*). This latter observation suggested that these chelators induced DNA damage or prevented DNA repair, as observed for the cytotoxic agent doxorubicin.

Considering the possible role of the redox activity of the Triapine-Fe complex in its antiproliferative activity, it was somewhat surprising to find that the compound showed selectivity against neoplastic cells compared with fibroblasts (Table 1; Fig. 2*B*). It can be suggested in neoplastic cells that an Fe pool must be present that is more susceptible to the action of Triapine than that of normal cells. The identity of this cellular Fe pool remains unknown at present and is the subject of ongoing investigations.

In terms of the biological targets of these ligands, our present studies directly demonstrate, using EPR spectroscopy, that both 311 and Triapine inhibit RR as part of their action. These results for 311 are supported by our previous studies, which demonstrated that this chelator acts to markedly inhibit [^{3}H]thymidine incorporation into DNA (37). Previous investigations have suggested that a major target of heterocyclic thiosemicarbazones, including Triapine, is RR (28, 63). In fact, the Fe complex of this class of compounds is far more effective at inhibiting RR than is the ligand alone (64, 65). Considering our results, the inhibition of RR by Triapine could be caused by two effects of this chelator. First, Triapine depletes intracellular Fe pools that may be used to supply the R2 subunit of RR; and, second, the subsequent formation of the Fe complex may then generate free radicals that damage RR and other vital molecules, *e.g.*, DNA. In this latter respect, Triapine appears similar to doxorubicin and bleomycin, both of which can redox cycle to generate free radicals after binding metal ions (57). Clearly, although the cytotoxicity and structures of 311 and Triapine are similar (Figs. 1 and 2), there is a marked difference in their mechanisms of action. Triapine has Fe chelation efficacy that is similar to that of DFO (Fig. 3) and is capable of generating reactive oxygen species after binding Fe (Fig. 6*B*). On the other hand, 311 has far greater Fe chelation activity than does either DFO or Triapine (Fig. 3) and forms an Fe complex that is redox-inactive (39).

For many years, the RR inhibitor, HU, has been used in the treatment of chronic myelocytic leukemia (66). However, HU has limited usefulness because of its short biological half-life, its relatively low affinity for RR, and the fact that resistance can develop against this agent (67–69). Nevertheless, the clinical usefulness of HU suggests that more effective RR inhibitors should have great potential as antineoplastic agents. Some Fe chelators are powerful inhibitors of RR because of their ability to bind Fe (6). Furthermore, specific Fe chelators can affect a variety of other metabolic pathways. For example, some ligands, such as 311, markedly inhibit Fe uptake from Tf and increase Fe mobilization from cells (36–38). Hence, the activity and potential of Fe chelators as antitumor agents are greater than those of HU.

Apart from the effect of the chelators on RR and Fe uptake from Tf and Fe mobilization from cells, it is of interest to note that DFO, Triapine, and 311 all decreased the phosphorylation of pRb and the expression of the cyclin D family (cyclin D1–D3) and also Cdk2 (Fig. 5*A*). All of these molecules are essential for G_1-S-phase progression and may be either direct or indirect targets of the ability of the ligands to bind cellular Fe pools.

In summary, the present study has demonstrated that the novel Fe chelator 311 shows selective antiproliferative activity against tumor cells that is similar to the activity of Triapine and much greater than that of DFO. In addition, we showed that Triapine acts as a chelator to increase Fe mobilization from cells and to prevent Fe uptake from Tf. However, the Fe chelation efficacy of Triapine is similar to that of DFO and much less than that of 311. Whereas the Fe complexes of 311 and DFO do not inhibit proliferation, the Triapine-Fe complex possesses pronounced antiproliferative activity, which may be related to its redox properties that result in the generation of cytotoxic free radicals.

ACKNOWLEDGMENTS

We kindly acknowledge many stimulating discussions with Professor Roger Dean and Dr. Mike Davies on the redox properties of these chelators.

REFERENCES

1. Hoffbrand, A. V., Ganeshaguru, K., Hooton, J. W. L., and Tatersall, M. H. N. Effect of iron deficiency and desferrioxamine on DNA synthesis in human cells. Br. J. Haematol., *33:* 517–526, 1976.

2. Bergeron, R. J., Cavanaugh, P. F. Jr., Kline, S. J., Hughes, R. G. Jr., Elliot, G. T., and Porter, C. W. Antineoplastic and antiherpetic activity of spermidine catecholamide iron chelators. Biochem. Biophys. Res. Commun., *121:* 848–854, 1984.

3. Hoyes, K. P., Hider, R. C., and Porter, J. B. Cell cycle synchronization and growth inhibition by 3-hydroxypyridin-4-one iron chelators in leukemic cell lines. Cancer Res., *52:* 4591–4599, 1992.

4. Seligman, P., Schleicher, R. B., Siriwardana, G., Domenico, J., and Gelfand, E. W. Effects of agents that inhibit cellular iron incorporation on bladder cell proliferation. Blood, *82:* 1608–1617, 1993.

5. Torti, S. V., Torti, F. M., Whitman, S. P., Brechbiel, M. W., Park, G., and Planalp, R. P. Tumor cell cytotoxicity of a novel metal chelator. Blood, *92:* 1384–1389, 1998.

6. Richardson, D. R. Iron chelators as effective anti-proliferative agents. Can. J. Physiol. Pharmacol., *75:* 1164–1180, 1997.

7. Larrick, J. W., and Cresswell, P. Modulation of cell surface iron transferrin receptors by cellular density and the state of activation. J. Supramol. Struct., *11:* 579–586, 1979.

8. Richardson, D. R., and Baker, E. Two mechanisms of iron uptake from transferrin by melanoma cells. The effect of desferrioxamine and ferric ammonium citrate. J. Biol. Chem., *267:* 13972–13979, 1992.

9. Richardson, D. R., and Baker, E. The uptake of iron and transferrin by the human melanoma cell. Biochim. Biophys. Acta, *1053:* 1–12, 1990.

10. Kemp, J. D., Thorson, J. A., Stewart, B. C., and Naumann, P. W. Inhibition of hematopoietic tumor growth by combined treatment with deferoxamine and an IgG monoclonal antibody against the Transferrin receptor: evidence for a threshold model of iron deprivation toxicity. Cancer Res., *52:* 4144–4148, 1992.

11. Kemp, J. D., Cardillo, T., Stewart, B. C., Kehrberg, E., Weiner, G., Hedland, B., and Naumann, P. W. Inhibition of lymphoma growth *in vivo* by combined treatment with hydroxyethyl starch deferoxamine conjugate and IgG monoclonal antibodies against the Transferrin receptor. Cancer Res., *55:* 3817–3824, 1995.

12. Chan, S. M., Hoffer, P. B., Maric, N., and Duray, P. Inhibition of gallium-67 uptake in melanoma by an anti-human Transferrin receptor monoclonal antibody. J. Nucl. Med., *28:* 1303–1307, 1987.

13. Chitamber, C. R., and Seligman, P. A. Effects of different Transferrin forms on Transferrin receptor expression, iron uptake, and cellular proliferation of human leukemic HL60 cells: mechanisms responsible for the specific cytotoxicity of Transferrin-gallium. J. Clin. Investig., *78:* 1538–1546, 1986.

14. Blatt, J., and Stitely, S. Antineuroblastoma activity of desferrioxamine in human cell lines. Cancer Res., *47:* 1749–1750, 1987.

15. Estrov, Z., Tawa, A., Wang, X-H., Dube, I. D., Sulh, H., Cohen, A., Gelfand, E. W., and Freedman, M. H. *In vivo* and *in vitro* effects of desferrioxamine in neonatal acute leukemia. Blood, *69:* 757–761, 1987.

16. Becton, D. L., and Bryles, P. Deferoxamine inhibition of human neuroblastoma viability and proliferation. Cancer Res., *48:* 7189–7192, 1988.

17. Donfrancesco, A., Deb, G., Dominici, C., Pileggi, D., Castello, M. A., and Helson, L. Effects of a single course of deferoxamine in neuroblastoma patients. Cancer Res., *50:* 4929–4930, 1990.

18. Donfrancesco, A., Deb, G., Dominici, C., Angioni, A., Caniglia, M., De Sio, L., Fidani, P., Amici, A., and Helson, L. Deferoxamine, cyclophosphamide, etoposide, carboplatin, and thiotepa (D-CECat): A new cytoreductive chelation-chemotherapy regimen in patients with advanced neuroblastoma. Am. J. Clin. Oncol., *15:* 319–322, 1992.

19. Donfrancesco, A., De Bernardi, B., Carli, M., Mancini, A., Nigro, M., De Sio, L., Casale, F., Bagnulo, S., Helson, L., and Deb, G. Deferoxamine (D) followed by cytoxan (C), etoposide (E), carboplatin (Ca), thio-TEPA (T), induction regimen in advanced neuroblastoma. Eur. J. Cancer, *31A:* 612–615, 1995.

20. Dezza, L., Cazzola, M., Danova, M., Carlo-Stella, C., Bergamaschi, G., Brugnatelli, S., Invernizzi, R., Mazzini, G., Riccardi, A., and Ascari, E. Effects of desferrioxamine on normal and leukemic human hematopoietic cell growth: *in vitro* and *in vivo* studies. Leukemia (Baltimore), *3:* 104–107, 1989.

21. Thelander, L., and Reichard, P. The reduction of ribonucleotides. Annu. Rev. Biochem., *48:* 133–158, 1979.

22. Cooper, C. E., Lynagh, G. R., Hoyes, K. P., Hider, R. C., Cammack, R., and Porter, J. B. The relationship of intracellular iron chelation to the inhibition and regeneration of human ribonucleotide reductase. J. Biol. Chem., *271:* 20291–20299, 1996.

23. Elford, H. L., Freese, M., Passamani, E., and Morris, H. P. Ribonucleotide reductase and cell proliferation. J. Biol. Chem., *245:* 5228–5233, 1970.

24. Weber, G. Enzymology of cancer cells. N. Engl. J. Med., *296:* 486–493, 1977.

25. Takeda, E., and Weber, G. Role of ribonucleotide reductase in expression in the neoplastic program. Life Sci., *28:* 1007–1014, 1981.

26. Witt, L., Yap, T., and Blakely, R. L. Regulation of ribonucleotide reductase activity and its possible exploitation in chemotherapy. Adv. Enzyme Regul., *17:* 157–171, 1979.

27. Agrawal, K. C., and Sartorelli, A. C. The chemistry and biological activity of α-(*N*)-heterocyclic carboxaldehyde thiosemicarbazones. Prog. Med. Chem., *15:* 321–356, 1978.

28. Finch, R. A., Liu, M-C., Grill, S. P., Rose, W. C., Loomis, R., Vasquez, K. M., Cheng, Y-C., and Sartorelli, A. C. Triapine (3-aminopyridine-2-carboxaldehyde-thiosemicarbazone): a potent inhibitor of ribonucleotide reductase activity with broad spectrum antitumor activity. Biochem. Pharmacol., *59:* 983–991, 2000.

29. French, F. A., and Blanz, E. J., Jr. The carcinostatic activity of α-(*N*)-heterocyclic carboxaldehyde thiosemicarbazones. I. Isoquinoline-1-carboxaldehyde thiosemicarbazone. Cancer Res., *25:* 1454–1458, 1965.

30. Levinson, W. E. Chelating substances. Antibiotics Chemother., *27:* 288–306, 1980.

31. Creasey, W. A., Agrawal, K. C., Capizzi, R. L., Stinson, K. K., and Sartorelli, A. C. Studies of the anti-neoplastic activity and metabolism of α-(*N*)-heterocyclic carboxaldehyde thiosemicarbazones in dogs and mice. Cancer Res., *32:* 565–572, 1972.

32. DeConti, R. C., Toftness, B. R., Agrawal, K. C., Tomchick, R., Mead, J. A. R., Bertino, J. R., Sartorelli, A. C., and Creasey, W. A. Clinical and pharmacological studies with 5-hydroxy-2-formylpyridine thiosemicarbazone. Cancer Res., *32:* 1455–1462, 1972.

33. Krakoff, I. H., Etcubanas, E., Tan, C., Mayer, K., Bethune, V., and Burchenai, J. H. Clinical trial of 5-hydroxypicolinaldehyde thiosemicar-

bazone (5-HP: NSC-107392), with special reference to its Fe chelating properties. Cancer Chemother. Rep., *53:* 207–212, 1974.

34. Liu, M. C., Lin, T. S., and Sartorelli, A. C. Synthesis and antitumor evaluation of amino derivatives of pyridine-2-carboxaldehyde thiosemicarbazone. J. Med. Chem., *35:* 3672–3677, 1992.

35. Cory, J. G., Cory, A. H., Rappa, G., Lorico, A., Liu, M. C., Lin, T. S., and Sartorelli, A. C. Inhibitors of ribonucleotide reductase. Comparative effects of amino- and hydroxy-substituted pyridine-2-carboxaldehyde thiosemicarbazones. Biochem. Pharmacol., *48:* 335–344, 1994.

36. Richardson, D. R., Tran, E., and Ponka, P. The potential of iron chelators of the pyridoxal isonicotinoyl hydrazone class as effective antiproliferative agents. Blood, *86:* 4295–4306, 1995.

37. Richardson, D. R., and Milnes, K. The potential of iron chelators of the pyridoxal isonicotinoyl hydrazone class as effective anti-proliferative agents II: The mechanism of action of ligands derived from salicylaldehyde benzoyl hydrazone and 2-hydroxy-1-naphthylaldehyde benzoyl hydrazone. Blood, *89:* 3025–3038, 1997.

38. Darnell, G., and Richardson, D. R. The potential of analogues of the pyridoxal isonicotinoyl hydrazone class as effective anti-proliferative agents III: the effect of the ligands on molecular targets involved in proliferation. Blood, *94:* 781–792, 1999.

39. Richardson, D. R., and Bernhardt, P. Crystal and molecular structure of 2-hydroxy-1-naphthylaldehyde isonicotinoyl hydrazone (NIH) and its iron(III) complex: an iron chelator with anti-proliferative activity. J. Biol. Inorg. Chem., *4*: 266–273, 1999.

40. Richardson, D. R. Cytotoxic analogues of the iron(III) chelator pyridoxal isonicotinoyl hydrazone: Effect of complexation with copper(II), gallium(III), and iron(III) on their anti-proliferative activity. Antimicrob. Agents Chemother., *41:* 2061–2063, 1997.

41. Gao, J., and Richardson, D. R. The potential of iron chelators of the pyridoxal isonicotinoyl hydrazone class as effective anti-proliferative agents IV. The mechanisms involved in inhibiting cell cycle progression. Blood, *98:* 842–850, 2001.

42. McCrohon, J. A., Jessup, W., Handelsman, D. J., and Celermeyer, D. S. Androgen exposure increases human monocyte adhesion to vascular endothelium and expression of vascular cell adhesion molecule-1. Circulation, *99*; 2317–2322, 1999.

43. Brown, A. J., Watts, G. F., Burnett, J. R., Dean, R. T., and Jessup, W. Sterol 27-hydroxylase acts on 7-ketocholestrol in human atherosclerotic lesions and macrophages in culture. J. Biol. Chem., *275*; 27627–27633, 2000.

44. Eaves, C. J. Assays of hemopoietic progenitor cells. *In*: E. Beutler, M. A. Lichtman, B. S. Coller, and T. J. Kipps (eds.), Williams Hematology, Vol. 5. New York: McGraw Hill, 1995.

45. Leibold, E. A., and Munro, H. N. Cytoplasmic protein binds *in vitro* to a highly conserved sequence in the 5′ untranslated region of ferritin heavy- and light-subunit mRNAs. Proc. Natl. Acad. Sci. USA, *85:* 2171–2175, 1988.

46. Müllner, E. W., Neupert, B., and Kühn, L. C. A specific mRNA binding factor regulates the iron-dependent stability of the cytoplasmic Transferrin receptor mRNA. Cell, *58:* 373–382, 1989.

47. Duling, D. R. Simulation of multiple isotropic spintrap EPR spectra. J. Magn. Reson., *104B:* 105–110, 1994.

48. Dean, R. T., and Nicholson, P. The action of nine chelators on iron-dependent radical damage. Free Radic. Res., *20:* 83–101, 1994.

49. Lovejoy, D. B., and Richardson, D. R. Novel "hybrid" iron chelators derived from aroylhydrazones and thiosemicarbazones demonstrate selective antiproliferative activity against tumor cells. Blood, *100:* 666–676, 2002.

50. Hermes-Lima, M., Nagy, E., Ponka, P., and Schulman, H. M. The iron chelator pyridoxal isonicotinoyl hydrazone (PIH) protects plasmid pUC-18 DNA against. OH-mediated strand breaks. Free Radic. Biol. Med., *25:* 875–880, 1998.

51. Sedlack, J., and Lindsay, R. Estimation of total, protein-bound, and nonprotein sulfhydryl groups in tissue with Ellman's reagent. Anal. Biochem., *25:* 192–205, 1968.

52. Olson, R. D., MacDonald, J. S., van Boxtel, C. J., Boerth, R. C., Harbison, R. D., Slonim, A. E., Freeman, R. W., and Oates, J. A. Regulatory role of glutathione and soluble sulfhydryl groups in the toxicity of Adriamycin. J. Pharmacol. Exp. Ther., *215:* 450–545, 1980.

53. Griffith, O. W., and Meister, A. Potent and specific inhibition of glutathione synthesis by buthionine sulfoximine (*s-n*-butyl homocysteine sulfoximine). J. Biol. Chem., *254:* 7558–7560, 1979.

54. Watts, R. N., and Richardson, D. R. Nitrogen monoxide (NO) and glucose. Unexpected links between energy metabolism and NO-mediated iron mobilization from cells. J. Biol. Chem., *276*: 4724–4732, 2001.

55. Olive, P. L. DNA precipitation assay: a rapid and simple method for detecting DNA damage in mammalian cells. Environ. Mol. Mutagen., *11:* 487–495, 1988.

56. Kulp, K. S., Green, S. L., and Vulliet, R. Iron deprivation inhibits cyclin-dependent kinase activity and decreases cyclin D/CDK protein levels in asynchronous MDA-MB-453 human breast cancer cells. Exp. Cell Res., *229:* 60–68, 1996.

57. Kwok, J., and Richardson, D. R. The cardioprotective effect of the iron chelator dexrazoxane (ICRF-187) on anthracycline-mediated cardiotoxicity. Redox Rep., *5:* 317–324, 2000.

58. Gutteridge, J. M. C. Ferrous-salt-promoted damage to deoxyribose and benzoate. Biochem. J., *243:* 709–714, 1987.

59. Singh, S., and Hider, R. C. Colorimetric detection of the hydroxyl radical: comparison of the hydroxyl-radical-generating ability of various iron complexes. Anal. Biochem., *171:* 47–54, 1988.

60. Richardson, D. R., Hefter, G. T., May, P. M., Webb, J., and Baker, E. Iron chelators of the pyridoxal isonicotinoyl hydrazone class III. Formation constants with calcium(II), magnesium(II) and zinc(II). Biol. Metals, *2:* 161–167, 1989.

61. Vitolo, L. M. W., Hefter, G. T., Clare, B. W., and Webb, J. Iron chelators of the pyridoxal isonicotinoyl hydrazone class. Part II. Formation constants with iron(III) and iron(II). Inorg. Chim. Acta, *170:* 171–176, 1990.

62. Antholine, W., Knight, J., Whelan, H., and Petering, D. H. Studies of the reaction of 2-formylpyridine thiosemicarbazone and its iron and copper complexes with biological systems. Mol. Pharmacol., *13:* 89–98, 1977.

63. Finch, R. A., Liu, M-C., Cory, A. H., Cory, J. G., and Sartorelli, A. C. Triapine (3-aminopyridine-2-carboxaldehyde thiosemicarbazone; 3-AP): An inhibitor of ribonucleotide reductase with antineoplastic activity. Adv. Enzyme Regul., *39:* 3–12, 1999.

64. Sartorelli, A. C., Agrawal, K. C., Tsiftsoglou, A. S., and Moore, E. C. Characterization of the biochemical mechanism of action of α-(*N*)-heterocyclic carboxaldehyde thiosemicarbazones. Adv. Enzyme Regul., *15:* 117–139, 1977.

65. Thelander, L., and Gräslund, A. Mechanism of inhibition of mammalian ribonucleotide reductase by the iron chelate of 1-formylisoquinoline thiosemicarbazone. J. Biol. Chem., *258:* 4063–4066, 1983.

66. Salmon, S. E. Part VII. Chemotherapeutic agents–cancer chemotherapy. *In*: F. H. Meyers, E. Jawetz, E. Goldfien and A. Goldfien, (eds.), Review of Medical Pharmacology, pp. 477–513. Los Altos, CA: Lange Medical Publications, 1980.

67. Beckloff, G. L., Lerner, H. J., Frost, D., Russo-Alesi, F. M., and Gitomer, S. Hydroxyurea (NSC-32065) in biological fluids: dose-concentration relationship. Cancer Chemother. Rep., *48:* 57–58, 1965.

68. Gwilt, P. R., and Tracewell, W. G. Pharmacokinetics and pharmacodynamics of hydroxyurea. Clin. Pharmacokinet., *34:* 347–358, 1998.

69. Moore, E. C., and Hurlbert, R. B. The inhibition of ribonucleoside diphosphate reductase by hydroxyurea, guanazole and pyrazoloimidazole (IMPY). *In*: J. G. Cory and A. H. Cory (eds.), Inhibitors of Ribonucleoside Diphosphate Reductase Activity, pp. 165–201. Oxford: Pergamon Press, 1989.